Journal of Alloys and Compounds 503 (2010) 209–212

Contents lists available at ScienceDirect

Journal of Alloys and Compounds

journal homepage: www.elsevier.com/locate/jallcom

Microstructure and piezoelectric properties of $Na_{0.5}K_{0.5}NbO_3$–$BiNiO_3$–$LiSbO_3$ lead-free ceramics

Chaoying Liu[a,*], Xinyu Liu[a,b], Minhong Jiang[b], Jiafeng Ma[a]

[a] Department of Information Material Science and Engineering, Guilin University of Electronic Technology, Guilin 541004, PR China
[b] College of Materials Science and Engineering, Central South University, Changsha 410083, PR China

ARTICLE INFO

Article history:
Received 24 February 2010
Received in revised form 26 April 2010
Accepted 28 April 2010
Available online 7 May 2010

Keywords:
Sodium potassium niobate
Piezoelectricity
Perovskite ceramics
Electrical properties

ABSTRACT

Lead-free $(0.94-x)Na_{0.5}K_{0.5}NbO_3$–$xBiNiO_3$–0.06$LiSbO_3$ piezoelectric ceramics have been sintered at 1105 °C by ordinary solid mixed oxide method. The phase transitional behavior and various electrical properties were investigated. All samples are typical ABO_3 style perovskite structure. A morphotropic phase boundary between orthorhombic and tetragonal ferroelectric phases has been identified in the composition range of $0.002 \le x \le 0.004$. Main piezoelectric parameters of these ceramics were optimized around $x = 0.002$ with an enhanced piezoelectric constant d_{33} of 240 pC N^{-1}, a planar electromechanical coefficient k_p of 44%, a mechanical factor Q_m of 38, and a Curie temperature T_c of 360 °C. These results indicate the materials studied have a promising future in a wide range of applications.

1. Introduction

Recently, solid solutions based on $Na_{0.5}K_{0.5}NbO_3$ (abbreviation NKN) have increasingly attracted the attention of researchers. Because of its relatively strong piezoelectric properties and highly Curie temperature, NKN-based ceramic systems were considered as one of the most promising candidates for lead-free piezoelectric applications. Pure NKN ceramics prepared from an ordinary mixed oxide root exhibit a low piezoelectric constant d_{33} of about 80 pC N^{-1} [1]. And the major disadvantage of pure NKN sintered in that way was the difficulty in obtaining dense enough ceramics [2]. Thus, oxides sintering aids (CuO, ZnO, MnO_2, etc.) or specialized sintering process were introduced to form liquid phases to prevent the pre-evaporation of Na_2O and lower the sintering temperature to overcome this drawback [3–7]. And perovskite compounds were widely introduced to form binary or ternary solid solutions to obtain industrial application suited lead-free piezoelectric ceramics as well [8–13]. And $(1-x)$NKN–$xLiSbO_3$ ceramics were reported to have high piezoelectric properties and the modification of $LiSbO_3$ optimized around $x = 0.04$–0.06 [10,14–16]. Meanwhile, searching for a solid solution system with a morphotropic phase boundary (MPB) was another aim of these efforts [14,17,18].

The aim of this work was to investigate the microstructure, dielectric and piezoelectric properties of $(0.94-x)Na_{0.5}K_{0.5}NbO_3$–$xBiNiO_3$–0.06$LiSbO_3$ ($(0.94-x)$NKN–xBN–LS6) ceramic systems prepared by ordinary mixed oxide sintering in air. The effect of low-content $BiNiO_3$ addition on the structure, phase transition behavior, and electrical properties of the $(0.94-x)$NKN–xBN–LS6 ceramic systems has also been closely studied.

2. Experimental procedures

$(0.94-x)$NKN–xBN–LS6 ($x = 0.002$, 0.004, 0.006, 0.008 and 0.01) ceramics were prepared by conventional mixed oxide sintering method. The raw materials were Na_2CO_3 (99.8%), K_2CO_3 (99%), Nb_2O_5 (99.5%), Bi_2O_3 (99.97%), NiO (99%), Li_2CO_3 (99%) and Sb_2O_3 (99.5%). All raw powders were separately dried in an oven at 80 °C for more than 24 h before batch weighing. These powders were weighted and then mixed by zirconia ball milling in ethanol for 12 h, then dried and calcined again at 850 °C for 6 h. The calcined powders were mixed with 3 wt.% polyvinyl alcohol (PVA) solution, and then pressed into pellets with a diameter of 18 mm under single direction pressure about 150 MPa. The green disks were sintered at 1105 °C for 2 h.

The phase structure of sintered ceramics was examined by X-ray diffraction (XRD, D8-2-Advanced, BRUKER AXS, German) with Cu-Kα radiation (2θ: 20–85°, step: 0.02°). Surface microstructure was observed by scanning electron microscopy (SEM, JSM-5610LV, JEOL, Japan). Density was measured by the Archimedes method with distilled water. Silver electrodes were screen-printed on both surfaces of each sintered disk by firing at 600 °C for 40 min. The samples were polarized in silicon oil for 10 min at 120 °C with poling fields 3–9 kV mm^{-1} applied direct on the two electrodes. Dielectric properties of the specimens were obtained together using an impedance analyzer (Agilent 4294A, Agilent Technologies, America) by measuring the capacitance and loss (Cp–D) of the specimen homogenously from 30 °C to 460 °C, using a heating rate of 60 °C h^{-1}. The piezoelectric coefficient (d_{33}) was recorded from 24-h-aged polarized samples using a quasistatic piezoelectric d_{33} meter (ZJ-3AN, Institute of Acoustics, Chinese Academy of Sciences, China). The planar coupling coefficient (k_p) and the mechanical quality factor (Q_m) were determined

* Corresponding author at: Guangxi Key Laboratory of Information Materials, Guilin University of Electronic Technology, Jinji Road No. 1, Guilin, Guangxi Province 541004, PR China. Tel.: +86 773 5605 346; fax: +86 773 5605 903.
E-mail address: leu.chaoying@gmail.com (C. Liu).

0925-8388/$ – see front matter © 2010 Elsevier B.V. All rights reserved.
doi:10.1016/j.jallcom.2010.04.234

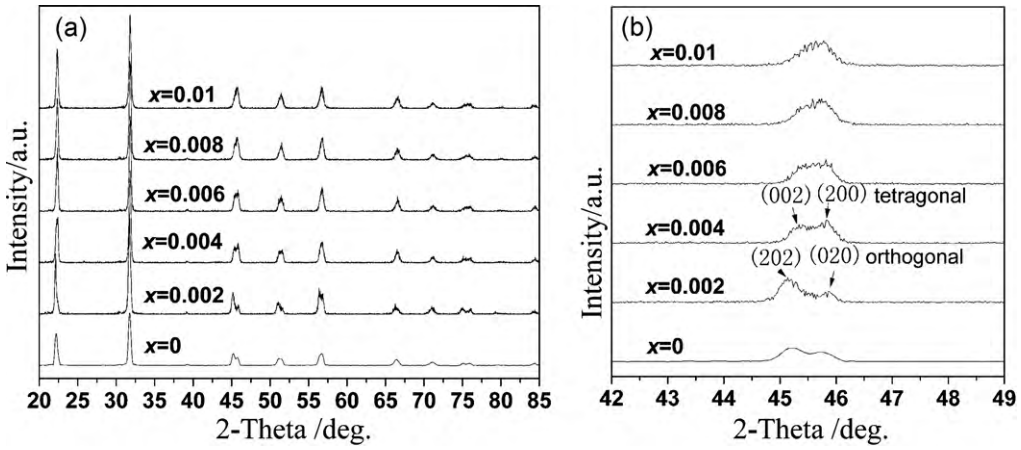

Fig. 1. X-ray diffraction patterns of $(0.96 - x)$NKN–xBN–LS6 ceramic systems at room temperature (25 °C).

by the resonance–anti-resonance technique using the impedance analyzer (Agilent 4294A).

3. Results and discussion

The XRD patterns at 2θ about 20–60° of sintered ceramics with different BN contents are shown in Fig. 1. A typical ABO_3 perovskite structure was well formed in all samples without any significant trace of other phases at room temperature. Pure KNN ceramic has an orthorhombic symmetry with the perovskite structure. And it was clear that the reflections at 2θ about 44.5–46.5° exhibit a feature of peak splitting and a shifting of the intensities of these peaks, which could be assigned to a phase transition between tetragonal phase with reflection peaks of (0 0 2)/(2 0 0)

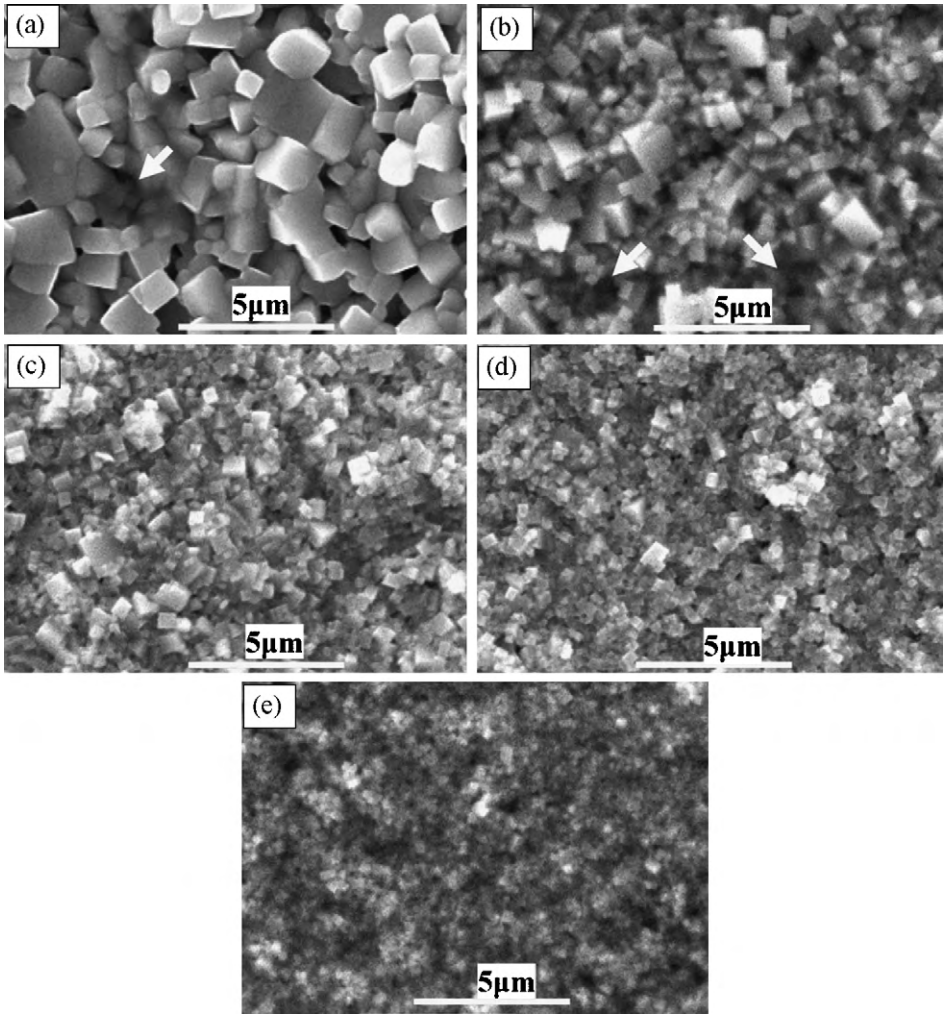

Fig. 2. Scanning electron microscopic (SEM) images of the $(0.96 - x)$NKN–xBN–LS6 ceramic systems sintered at 1105 °C (a) $x = 0.002$, (b) $x = 0.004$, (c) $x = 0.006$, (d) $x = 0.008$, and (e) $x = 0.01$.

Table 1
Density and electrical properties of KNN–*x*BN–LS6 ceramics.

	x					
	0 [25]	0.002	0.004	0.006	0.008	0.1
Bulk density ($g\,cm^{-3}$)	4.40	4.43	4.39	4.31	4.33	4.26
Poling electric field ($kV\,mm^{-1}$)	–	3.987	4.663	4.717	7.445	8.796
d_{33} ($pC\,N^{-1}$)	212	240	195	185	105	60
k_p	0.46	0.44	0.42	0.38	0.24	0.15
Q_m	40[a]	37	55	75	80	96
T_c (°C)	358	360	340	330	325	305

[a] Q_m data was quoted from Ref. [26].

and orthorhombic phase with reflection peaks of (2 0 2)/(0 2 0) as BN content decreased from $x = 0.004$ to $x = 0.002$, indicating a MPB between tetragonal phase to orthorhombic phase occurred in the composition range of $x = 0.002$ to $x = 0.004$. The above-mentioned phase transition can be more clearly seen in Fig. 1(b). In the $(K_{0.5}Na_{0.5})_{1-x}Li_x(Nb_{1-y}Sb_y)O_3$ with $y = 0.06$ and $x = 0.06$ [19] and $(K_{0.5}Na_{0.5})_{0.90}Li_{0.06}Sr_{0.02}Nb_{(1-x)}Sb_xO_3$ with $x = 0.06$ [20], the crystalline symmetry is tetragonal. But the crystalline symmetry of the $(1-x)$ $(0.95Na_{0.5}K_{0.5}NbO_3–0.05LiSbO_3)–xBiFeO_3$ with $x = 0.00$ is orthorhombic symmetry [14]. In these works, almost the same composition, but led to quite different crystalline symmetry, this may be a result of different sample preparing routes. It was considered the crystal structure of these ceramics was sensitive even with a small change in compositions, which presented an effective method for controlling the crystal structure of $(0.94-x)$NKN–*x*BN–LS6 ceramics.

Fig. 2 shows the SEM surface micrographs of the $(0.94-x)$NKN–*x*BN–LS6 ceramic samples modified with LS and different content of BN sintered at optimum temperature of 1105 °C for 2 h. It can be observed that all samples have dense microstructures and a typical feature of quadrate shape, which was common in NKN-based ceramics [5,16,21,22]. The addition of BN has significant effect on the sintering behavior and the morphology features of $(0.94-x)$NKN–*x*BN–LS6 ceramics. With increasing BN content, the growth of grain restrained and the microstructure uniformity of $(0.94-x)$NKN–*x*BN–LS6 ceramics decreased which was mainly because of the increasing Ni-based compositions introduced by BN content. Besides, liquid phase traces identified by the arrows in Fig. 2(a) and (b) were found in these images, which can be explained by the introduction of low-melting point of Bi_2O_3- and $LiSbO_3$-based phases. The formation of liquid phase has significant impact in improving the density and the grain growth process of the $(0.94-x)$NKN–*x*BN–LS6 ceramics. With the increasing of BN content, the content of liquid phase decreased and finally disappeared after $x \geq 0.006$ and the mean grain size of these specimens obviously decreased from about 2 μm to 0.4 μm, which may be a result of the contribution of the increasing of relevant high-melting point of NiO-based compositions. Otherwise, the Bi ions doping in the NKN–LS ceramics are coupled with that of Ni ions, they both take part in affecting the microstructure of NKN–LS ceramics. When the content of BN is small enough, they both are positive for the improvement of density and for the increase in content of liquid phase in NKN–LS ceramics, but once if the amount of Ni ions reached a limit which is located around $x = 0.002$, their contribution reverse to be negative. It is easy to get that excess BN addition introduction of Ni-based compositions caused a decrease of the grain size, which can result in the decrease of the bulk density. As BN addition increased, both the content of liquid phases and Ni-based high-melting-point phase increased. The increased content of liquid phase brings a well environment for large-sized crystal growth. But the increasing of Ni-based high-melting-point phase introduced more numbers of dispersion grain nucleus, which would restrain the growth of crystals. The composition of liquid phase changes dynamic during sintering process. It is possible that there maybe a complicated balance between the grain size and the composition changes in liquid phase which remains a problem for further research.

Table 1 presents the main dielectric and piezoelectric parameters of $(0.94-x)$NKN–*x*BN–LS6 ceramics. The electrical properties of $(0.94-x)$NKN–*x*BN–LS6 ceramics have a strong dependence on the compositions. With the increasing of BN content, the T_c, d_{33} and k_p decreased from 360 °C, 240 $pC\,N^{-1}$ and 44% to 305 °C, 60 $pC\,N^{-1}$ and 16%, respectively, while the variation of the Q_m was the opposite, that is, increased from 38 to 97. The enhanced properties may be attributed to the ease of domain wall movement around the MPB, due to the coexistence of the orthorhombic and tetragonal phases in this system [23,24]. The domain rotation in the polarizing process may be easier for ceramics with improved bulk density and optimized grain size.

Fig. 3 shows the temperature dependence of relevant dielectric constant (ε_r) and dielectric loss ($\tan\delta$) measured at 10 kHz

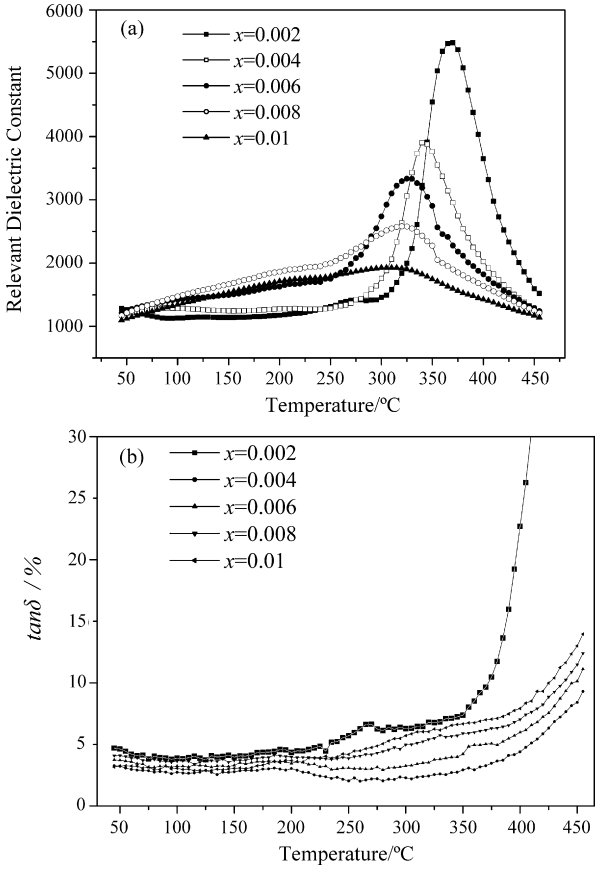

Fig. 3. Temperature dependence of $(0.96-x)$NKN–xBN–LS6 ceramic systems sintered at 1105 °C (30–460 °C). (a) Dielectric spectroscopy and (b) dielectric Loss.

for $(0.94-x)$NKN–xBN–LS6 ceramics in the range of 30–460 °C. The addition of BN influences obviously the dielectric properties of $(0.94-x)$NKN–xBN–LS6 ceramics. The variations of T_c which corresponds with the transitions from tetragonal to cubic phase was affected by the amount of BN addition in a very orderliness way (as showed in Table 1). It is obvious from Fig. 3(a) that both of the T_c (the peaks around 350 °C) and the dielectric constant peaks orderly and gradually decreased from about 360 °C to 300 °C with the increasing of BN content from $x = 0.002$–0.01. This may be a result of a homogeneous diffusion process, which was based on the addition of BN. The content of BN was diffused to the crystal lattice homogeneously at all of these addition levels. And the $(0.94-x)$NKN–xBN–LS6 ($x \leq 0.006$) ceramics showed typical temperature dependence of the dielectric constant curves with common NKN-based lead-free ceramics [14,25,27–29], however the $(0.94-x)$NKN–xBN–LS6 ($x \geq 0.006$) ceramics presented a feature like diffusion phase transition, and their intensity of peaks at around 300 °C were largely induced. Moreover, in Fig. 3 (b), it can be obviously seen that the dielectric loss of all the samples was low at 30–375 °C. Furthermore, the loss of all these samples was lower than 5% at 30–200 °C and no more than 10% over the T_c, the relevant low dielectric loss may be a result of the density improvement due to the additions of BN and LS.

4. Conclusions

$(0.94-x)$NKN–xBN–LS6 solid solution ceramic systems with typical perovskite structure and good piezoelectric properties were prepared by conventional mix-oxide sintering method. The small amount of BN (≤1%) introduced a significant change on the crystal structure and the electrical properties of $(0.94-x)$NKN–xBN–LS6 ceramics. A morphotropic phase boundary between orthogonal phase and tetragonal phase was attained between $x = 0.002$ and $x = 0.004$. Main piezoelectric parameters were optimized nearly at $x = 0.002$ with d_{33}, Q_m and k_p of 240 pC N^{-1}, 38 and 44%, and a relevant high Curie temperature of 350 °C, showing a promising future as lead-free ceramics for a wide range of applications.

Acknowledgements

The authors wish to acknowledge the financial support of the Guangxi Key Laboratory of Information Materials Fund. We would like to thank Mr. Jun Chen and Ms. Xiujuan Zhou for support in the X-ray and SEM analysis of selected samples.

References

[1] L. Egerton, D.M. Dillon, J. Am. Ceram. Soc. 42 (1959) 438–442.
[2] M. Demartin Maeder, D. Damjanovic, N. Setter, J. Electro. Ceram. (2004) 385–392.
[3] R. Zuo, B. Ma, Y. Liu, Z. Xu, J. Alloys Compd. 488 (2009) 465–468.
[4] H.E. Mgbemere, R.-P. Herber, G.A. Schneider, J. Eur. Ceram. Soc. 29 (2009) 1729–1733.
[5] J.G. Fisher, S.-J.L. Kang, J. Eur. Ceram. Soc. 29 (2009) 2581–2588.
[6] E. Atamanik, V. Thangadurai, Mater. Res. Bull. 44 (2009) 931–936.
[7] F. Rubio-Marcos, J.J. Romero, M.G. Navarro-Rojero, J.F. Fernandez, J. Eur. Ceram. Soc. 29 (2009) 3045–3052.
[8] Y.G. Lv, C.L. Wang, J.L. Zhang, L. Wu, M.L. Zhao, J.P. Xu, Mater. Res. Bull. 44 (2009) 284–287.
[9] X.-P. Jiang, Q. Yang, Z.-D. Yu, F. Hu, C. Chen, N. Tu, Y.-M. Li, J. Alloys Compd. 493 (2010) 276–280.
[10] L. Chen, H. Fan, M. Zhang, C. Yang, X. Chen, J. Alloys Compd. 492 (2010) 313–319.
[11] Y. Wang, J. Wu, D. Xiao, W. Wu, B. Zhang, J. Zhu, P. Yu, L. Wu, J. Alloys Compd. 472 (2009) L6–L8.
[12] M. Sutapun, C.-C. Huang, D.P. Cann, N. Vittayakorn, J. Alloys Compd. 479 (2009) 462–466.
[13] J. Hao, Z. Xu, R. Chu, W. Li, G. Li, Q. Yin, J. Alloys Compd. 484 (2009) 233–238.
[14] M. Jiang, X. Liu, G. Chen, Scripta Mater. 60 (2009) 909–912.
[15] W. Jiagang, X. Dingquan, W. Yuanyu, Z. Jianguo, Y. Ping, J. Yihang, J. Appl. Phys. 102 (2007) 114111–114113.
[16] J. Wu, D. Xiao, Y. Wang, J. Zhu, W. Shi, W. Wu, B. Zhang, J. Li, J. Alloys Compd. 476 (2009) 782–786.
[17] C. Wang, Y.-D. Hou, H.-Y. Ge, M.-K. Zhu, H. Yan, J. Eur. Ceram. Soc. 29 (2009) 2589–2594.
[18] Y. Guo, K.-i. Kakimoto, H. Ohsato, Mater. Lett. 59 (2005) 241–244.
[19] D. Lin, K.W. Kwok, K.H. Lam, H.L.W. Chan, J. Phys. D: Appl. Phys. 40 (2007) 3500–3505.
[20] Z. Yang, Y. Chang, B. Liu, L. Wei, Mater. Sci. Eng. A 432 (2006) 292–298.
[21] S.-H. Park, C.-W. Ahn, S. Nahm, J.-S. Song, Jpn. J. Appl. Phys. 43 (2004) L1072–L1074.
[22] S. King, J. Shen, J. Am. Ceram. Soc. 73 (1990) 1449–1450.
[23] M. Jiang, X. Liu, C. Liu, Mater. Res. Bull. 45 (2010) 220–223.
[24] F. Rubio-Marcos, J.J. Romero, D.A. Ochoa, J.E. Garcia, R. Perez, J.F. Fernandez, J. Am. Ceram. Soc. 93 (2010) 318–321.
[25] D. Lin, K.W. Kwok, K.H. Lam, H.L.W. Chan, J. Appl. Phys. 101 (2007) 074111–074116.
[26] S. Zhang, R. Xia, T.R. Shrout, G. Zang, J. Wang, Solid State Commun. 141 (2007) 675–679.
[27] M. Jiang, X. Liu, G. Chen, C. Zhou, Mater. Lett. 63 (2009) 1262–1265.
[28] R. Zuo, J. Rodel, R. Chen, L. Li, J. Am. Ceram. Soc. 89 (2006) 2010–2015.
[29] W. Jiagang, W. Yuanyu, X. Dingquan, Z. Jianguo, Y. Ping, W. Lang, W. Wenjuan, Jpn. J. Appl. Phys. 46 (2007) 7375–7377.